



Branching Fraction, Polarization and CP -Violating Asymmetries in $B^0 \rightarrow D^{*+} D^{*-}$ Decays

Belle Collaboration

H. Miyake^{ac}, M. Hazumi^g, K. Abe^g, K. Abe^{an}, H. Aihara^{ap},
Y. Asano^{at}, V. Aulchenko^a, T. Aushev^k, T. Aziz^{al},
S. Bahinipati^d, A. M. Bakich^{ak}, V. Balagura^k, Y. Ban^{ae},
S. Banerjee^{al}, A. Bay^p, I. Bedny^a, U. Bitenc^l, I. Bizjak^l,
S. Blyth^x, A. Bondar^a, A. Bozek^y, M. Bračko^{g,r,l},
J. Brodzicka^y, T. E. Browder^f, Y. Chao^x, A. Chen^v,
K.-F. Chen^x, B. G. Cheon^c, R. Chistov^k, S.-K. Choi^e,
Y. Choi^{aj}, Y. K. Choi^{aj}, A. Chuvikov^{af}, J. Dalseno^s,
M. Danilov^k, M. Dash^{au}, L. Y. Dongⁱ, J. Dragic^s,
A. Drutskoy^d, S. Eidelman^a, V. Eiges^k, Y. Enari^t, S. Fratina^l,
N. Gabyshev^a, A. Garmash^{af}, T. Gershon^g, G. Gokhroo^{al},
B. Golob^{q,l}, J. Haba^g, K. Hara^g, T. Hara^{ac}, N. C. Hastings^g,
K. Hayasaka^t, H. Hayashii^u, L. Hinz^p, T. Hokuue^t, Y. Hoshi^{an},
S. Hou^v, W.-S. Hou^x, T. Iijima^t, A. Imoto^u, K. Inami^t,
A. Ishikawa^g, R. Itoh^g, M. Iwasaki^{ap}, Y. Iwasaki^g,
J. H. Kang^{av}, J. S. Kangⁿ, P. Kapusta^y, S. U. Kataoka^u,
N. Katayama^g, H. Kawai^b, T. Kawasaki^{aa}, H. R. Khan^{aq},
H. Kichimi^g, H. J. Kim^o, J. H. Kim^{aj}, S. K. Kim^{ai},
S. M. Kim^{aj}, K. Kinoshita^d, P. Koppenburg^g, S. Korpar^{r,l},
P. Križan^{q,l}, P. Krokovny^a, R. Kulasiri^d, C. C. Kuo^v,
A. Kuzmin^a, Y.-J. Kwon^{av}, G. Leder^j, S. E. Lee^{ai}, T. Lesiak^y,
J. Li^{ah}, S.-W. Lin^x, D. Liventsev^k, G. Majumder^{al}, F. Mandl^j,
T. Matsumoto^{ar}, A. Matyja^y, W. Mitaroff^j, K. Miyabayashi^u,
H. Miyata^{aa}, R. Mizuk^k, D. Mohapatra^{au}, T. Mori^{aq},

T. Nagamine^{ao}, Y. Nagasaka^h, E. Nakano^{ab}, M. Nakao^g,
H. Nakazawa^g, Z. Natkaniec^y, S. Nishida^g, O. Nitoh^{as},
S. Ogawa^{am}, T. Ohshima^t, T. Okabe^t, S. Okuno^m,
S. L. Olsen^f, W. Ostrowicz^y, H. Ozaki^g, P. Pakhlov^k,
H. Palka^y, H. Park^o, N. Parslow^{ak}, L. S. Peak^{ak}, R. Pestotnik^ℓ,
L. E. Piilonen^{au}, M. Rozanska^y, H. Sagawa^g, Y. Sakai^g,
N. Sato^t, T. Schietinger^p, O. Schneider^p, P. Schönmeier^{ao},
J. Schümann^x, C. Schwanda^j, A. J. Schwartz^d, K. Senyo^t,
R. Seuster^f, M. E. Seviour^s, H. Shibuya^{am}, J. B. Singh^{ad},
A. Somov^d, N. Soni^{ad}, R. Stamen^g, S. Stanič^{at,1}, M. Starič^ℓ,
T. Sumiyoshi^{ar}, S. Suzuki^{ag}, S. Y. Suzuki^g, O. Tajima^g,
F. Takasaki^g, K. Tamai^g, N. Tamura^{aa}, M. Tanaka^g,
Y. Teramoto^{ab}, X. C. Tian^{ae}, K. Trabelsi^f, T. Tsukamoto^g,
S. Uehara^g, K. Ueno^x, T. Uglov^k, S. Uno^g, Y. Ushiroda^g,
G. Varner^f, K. E. Varvell^{ak}, S. Villa^p, C. C. Wang^x,
C. H. Wang^w, M.-Z. Wang^x, M. Watanabe^{aa}, Y. Watanabe^{aq},
A. Yamaguchi^{ao}, H. Yamamoto^{ao}, T. Yamanaka^{ac},
Y. Yamashita^z, M. Yamauchi^g, J. Ying^{ae}, Y. Yusa^{ao},
J. Zhang^g, L. M. Zhang^{ah}, Z. P. Zhang^{ah}, V. Zhilich^a, and
D. Žontar^{q,ℓ}

^a*Budker Institute of Nuclear Physics, Novosibirsk, Russia*

^b*Chiba University, Chiba, Japan*

^c*Chonnam National University, Kwangju, South Korea*

^d*University of Cincinnati, Cincinnati, OH, USA*

^e*Gyeongsang National University, Chinju, South Korea*

^f*University of Hawaii, Honolulu, HI, USA*

^g*High Energy Accelerator Research Organization (KEK), Tsukuba, Japan*

^h*Hiroshima Institute of Technology, Hiroshima, Japan*

ⁱ*Institute of High Energy Physics, Chinese Academy of Sciences, Beijing, PR
China*

^j*Institute of High Energy Physics, Vienna, Austria*

^k*Institute for Theoretical and Experimental Physics, Moscow, Russia*

^ℓ*J. Stefan Institute, Ljubljana, Slovenia*

^m*Kanagawa University, Yokohama, Japan*

ⁿ*Korea University, Seoul, South Korea*

^o*Kyungpook National University, Taegu, South Korea*

^p*Swiss Federal Institute of Technology of Lausanne, EPFL, Lausanne, Switzerland*

^q*University of Ljubljana, Ljubljana, Slovenia*

^r*University of Maribor, Maribor, Slovenia*

^s*University of Melbourne, Victoria, Australia*

^t*Nagoya University, Nagoya, Japan*

^u*Nara Women's University, Nara, Japan*

^v*National Central University, Chung-li, Taiwan*

^w*National United University, Miao Li, Taiwan*

^x*Department of Physics, National Taiwan University, Taipei, Taiwan*

^y*H. Niewodniczanski Institute of Nuclear Physics, Krakow, Poland*

^z*Nihon Dental College, Niigata, Japan*

^{aa}*Niigata University, Niigata, Japan*

^{ab}*Osaka City University, Osaka, Japan*

^{ac}*Osaka University, Osaka, Japan*

^{ad}*Panjab University, Chandigarh, India*

^{ae}*Peking University, Beijing, PR China*

^{af}*Princeton University, Princeton, NJ, USA*

^{ag}*Saga University, Saga, Japan*

^{ah}*University of Science and Technology of China, Hefei, PR China*

^{ai}*Seoul National University, Seoul, South Korea*

^{aj}*Sungkyunkwan University, Suwon, South Korea*

^{ak}*University of Sydney, Sydney, NSW, Australia*

^{al}*Tata Institute of Fundamental Research, Bombay, India*

^{am}*Toho University, Funabashi, Japan*

^{an}*Tohoku Gakuin University, Tagajo, Japan*

^{ao}*Tohoku University, Sendai, Japan*

^{ap}*Department of Physics, University of Tokyo, Tokyo, Japan*

^{aq}*Tokyo Institute of Technology, Tokyo, Japan*

^{ar}*Tokyo Metropolitan University, Tokyo, Japan*

^{as}*Tokyo University of Agriculture and Technology, Tokyo, Japan*

^{at}*University of Tsukuba, Tsukuba, Japan*

^{au}*Virginia Polytechnic Institute and State University, Blacksburg, VA, USA*

^{av}*Yonsei University, Seoul, South Korea*

Abstract

We present measurements of the branching fraction, the polarization parameters and CP -violating asymmetries in $B^0 \rightarrow D^{*+}D^{*-}$ decays using a 140 fb^{-1} data sample collected at the $\Upsilon(4S)$ resonance with the Belle detector at the KEKB energy-asymmetric e^+e^- collider. We obtain $\mathcal{B}(B^0 \rightarrow D^{*+}D^{*-}) = [0.81 \pm 0.08(\text{stat}) \pm 0.11(\text{syst})] \times 10^{-3}$, $R_{\perp} = 0.19 \pm 0.08(\text{stat}) \pm 0.01(\text{syst})$, $R_0 = 0.57 \pm 0.08(\text{stat}) \pm 0.02(\text{syst})$, $\mathcal{S} = -0.75 \pm 0.56(\text{stat}) \pm 0.12(\text{syst})$ and $\mathcal{A} = -0.26 \pm 0.26(\text{stat}) \pm 0.06(\text{syst})$. Consistency with Standard Model expectations is also discussed.

Key words: B decay, CP violation, $\sin 2\phi_1$

PACS: 11.30.Er, 12.15.Ff, 13.25.Hw

1 Introduction

In the Standard Model (SM), CP violation arises from an irreducible complex phase, the Kobayashi-Maskawa (KM) phase [1], in the weak-interaction quark-mixing matrix. In particular, the SM predicts CP asymmetries in the time-dependent rates for B^0 and \overline{B}^0 decays to a common CP eigenstate f_{CP} [2]. Recent measurements of the CP -violation parameter $\sin 2\phi_1$ by the Belle [3,4] and BaBar [5] collaborations established CP violation in $B^0 \rightarrow J/\psi K_S^0$ and related decay modes [6], which are governed by the $b \rightarrow c\bar{c}s$ transition, at a level consistent with KM expectations. Here ϕ_1 is one of the three interior angles of the Unitarity Triangle [3,4].

Despite this success, many tests remain before it can be concluded that the KM phase is the only source of CP violation. The $B^0 \rightarrow D^{*+}D^{*-}$ decay, which is dominated by the $b \rightarrow c\bar{c}d$ transition, provides an additional test of the SM. Within the SM, measurements of CP violation in this mode should yield the $\sin 2\phi_1$ value to a good approximation if the contribution from the penguin diagram is neglected. The correction from the penguin diagram is expected to be small [7]. Thus, a significant deviation in the time-dependent CP asymmetry in these modes from what is observed in $b \rightarrow c\bar{c}s$ decays would be evidence for a new CP -violating phase.

In the decay chain $\Upsilon(4S) \rightarrow B^0\overline{B}^0 \rightarrow f_{CP}f_{\text{tag}}$, where one of the B mesons decays at time t_{CP} to a final state f_{CP} and the other decays at time t_{tag} to a final state f_{tag} that distinguishes between B^0 and \overline{B}^0 , the decay rate has a time dependence given by [2]

$$\mathcal{P}(\Delta t) = \frac{e^{-|\Delta t|/\tau_{B^0}}}{4\tau_{B^0}} \left\{ 1 + q \left[\mathcal{S} \sin(\Delta m_d \Delta t) + \mathcal{A} \cos(\Delta m_d \Delta t) \right] \right\}. \quad (1)$$

¹ on leave from Nova Gorica Polytechnic, Nova Gorica, Slovenia

Here \mathcal{S} and \mathcal{A} are CP -violation parameters, τ_{B^0} is the B^0 lifetime, Δm_d is the mass difference between the two B^0 mass eigenstates, $\Delta t = t_{CP} - t_{\text{tag}}$, and $q = +1$ (-1) when the tagging B meson is a B^0 (\bar{B}^0). The parameter \mathcal{S} corresponds to the mixing-induced CP violation and is related to $\sin 2\phi_1$, while \mathcal{A} represents direct CP violation that normally arises from the interference between tree and penguin diagrams.

In $B^0 \rightarrow D^{*+}D^{*-}$ decays the final state D^* mesons may be in a state of s -, p - or d -wave relative orbital angular momentum. Since s - and d -waves are even under the CP transformation while the p -wave is odd, the CP -violation parameters in Eq. (1) are diluted. In order to determine the dilution, one needs to measure the CP -odd fraction. This can be accomplished with a time-integrated angular analysis. The BaBar collaboration has measured the polarization and CP asymmetries [8], and find the CP -odd contribution to be small, consistent with theoretical expectations [7]. The CP asymmetries are found to differ slightly from the expectation that neglects the contribution from the penguin diagram.

In this Letter we report measurements of the branching fraction, the polarization parameters and CP asymmetries in $B^0 \rightarrow D^{*+}D^{*-}$ decays based on a 140 fb^{-1} data sample, which corresponds to 152 million $B\bar{B}$ pairs. At the KEKB energy-asymmetric e^+e^- (3.5 on 8.0 GeV) collider [9], the $\Upsilon(4S)$ is produced with a Lorentz boost of $\beta\gamma = 0.425$ antiparallel to the positron beamline (z). Since the B^0 and \bar{B}^0 mesons are approximately at rest in the $\Upsilon(4S)$ center-of-mass system (cms), Δt can be determined from the displacement in z between the f_{CP} and f_{tag} decay vertices: $\Delta t \simeq (z_{CP} - z_{\text{tag}})/(\beta\gamma c) \equiv \Delta z/(\beta\gamma c)$.

The Belle detector [10] is a large-solid-angle spectrometer that includes a three-layer silicon vertex detector (SVD), a 50-layer central drift chamber (CDC), an array of aerogel threshold Cherenkov counters (ACC), time-of-flight (TOF) scintillation counters, and an electromagnetic calorimeter comprised of CsI(Tl) crystals (ECL) located inside a superconducting solenoid coil that provides a 1.5 T magnetic field. An iron flux-return located outside of the coil is instrumented with resistive plate chambers to detect K_L^0 mesons and to identify muons (KLM).

2 Event Selection

We reconstruct $B^0 \rightarrow D^{*+}D^{*-}$ decays in the following D^* final states; ($D^0\pi^+$, $\bar{D}^0\pi^-$), ($D^0\pi^+$, $D^-\pi^0$) and ($D^+\pi^0$, $\bar{D}^0\pi^-$). For the D^0 decays we use $D^0 \rightarrow K^-\pi^+$, $K^-\pi^+\pi^0$, $K^-\pi^+\pi^+\pi^-$, K^+K^- , $K_S^0\pi^+\pi^-$ and $K_S^0\pi^+\pi^-\pi^0$. For the D^+ decays we use $D^+ \rightarrow K_S^0\pi^+$, $K_S^0\pi^+\pi^0$, $K_S^0K^+$, $K^-\pi^+\pi^+$ and $K^-K^+\pi^+$. We allow all combinations of D decays except for cases where both D decays

include neutral kaons in the final state.

Charged tracks from D meson decays are required to be consistent with originating from the interaction point (IP). Charged kaons are separated from pions according to the likelihood ratio $P_{K/\pi} \equiv \mathcal{L}(K)/[\mathcal{L}(K) + \mathcal{L}(\pi)]$, where the likelihood function \mathcal{L} is based on the combined information from the ACC, CDC dE/dx and TOF measurements. We require $P_{K/\pi} > 0.1$ (0.2) for kaons in 2-prong (4-prong) D meson decays. The kaon identification efficiency is 96%, and 13% of pions are misidentified as kaons. Candidate charged pions are required to satisfy $P_{K/\pi} < 0.9$, which provides a pion selection efficiency of 91% with a kaon misidentification probability of 3%. Neutral pions are formed from two photons with invariant masses above $119 \text{ MeV}/c^2$ and below $146 \text{ MeV}/c^2$. To reduce the background from low-energy photons, we require $E_\gamma > 0.03 \text{ GeV}$ for each photon and $p_{\pi^0} > 0.1 \text{ GeV}/c$, where E_γ and p_{π^0} are the photon energy and the π^0 momentum in the laboratory frame, respectively. Candidate $K_S^0 \rightarrow \pi^+\pi^-$ decays are reconstructed from oppositely charged track pairs that have invariant masses within $15 \text{ MeV}/c^2$ of the nominal K_S^0 mass. A reconstructed K_S^0 is required to have a displaced vertex and a flight direction consistent with that of a K_S^0 originating from the IP.

Candidate D mesons are reconstructed from the selected kaons and pions, and are required to have invariant masses within 6σ (3σ) of the D meson mass for 2-prong (3- or 4-prong) decays, where σ is the mass resolution that ranges from 5 to $10 \text{ MeV}/c^2$. In this selection σ is obtained by fitting the Monte Carlo (MC) simulated D meson mass. These D^0 (D^+) candidates are then combined with π^+ (π^0) to form D^{*+} candidates, where the IP and pion identification requirements are not used to select π^+ candidates. The mass difference between D^{*+} and D^0 (D^+) is required to be within 3.00 (2.25) MeV/c^2 of the nominal mass difference. We identify B meson decays using the energy difference $\Delta E \equiv E_B^{\text{cms}} - E_{\text{beam}}^{\text{cms}}$ and the beam-energy constrained mass $M_{\text{bc}} \equiv \sqrt{(E_{\text{beam}}^{\text{cms}})^2 - (p_B^{\text{cms}})^2}$, where $E_{\text{beam}}^{\text{cms}}$ is the beam energy in the cms, and E_B^{cms} and p_B^{cms} are the cms energy and momentum, respectively, of the reconstructed B candidate. The B meson signal region is defined as $|\Delta E| < 0.04 \text{ GeV}$ and M_{bc} within 3σ of the B meson mass, where σ is $3.5 \text{ MeV}/c^2$. In order to suppress background from the $e^+e^- \rightarrow u\bar{u}$, $d\bar{d}$, $s\bar{s}$, or $c\bar{c}$ continuum, we require $H_2/H_0 < 0.4$, where H_2 (H_0) is the second (zeroth) Fox-Wolfram moment [11]. After applying this requirement, we find that the contributions to the background from B^+B^- , $B^0\bar{B}^0$ and continuum are approximately equal. Figure 1 shows the M_{bc} and ΔE distributions for the $B^0 \rightarrow D^{*+}D^{*-}$ candidates that are in the ΔE and M_{bc} signal regions, respectively. In the M_{bc} and ΔE signal regions there are 194 events.

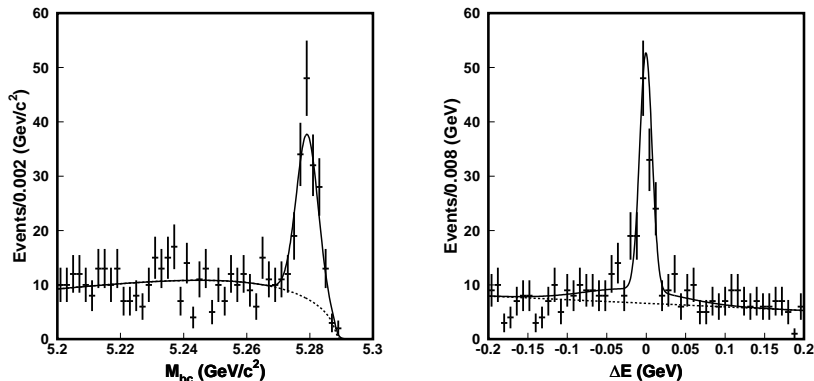


Fig. 1. (Left) M_{bc} and (right) ΔE distributions for $B^0 \rightarrow D^{*+}D^{*-}$ candidates within the ΔE (M_{bc}) signal region. Solid curves show the fit to signal plus background distributions, and dashed curves show the background contributions that comprise B^+B^- , $B^0\bar{B}^0$ and continuum events.

3 Branching Fraction

To determine the signal yield, we perform a two-dimensional maximum likelihood fit to the M_{bc} - ΔE distribution ($5.2 \text{ GeV}/c^2 < M_{bc} < 5.3 \text{ GeV}/c^2$ and $|\Delta E| < 0.2 \text{ GeV}$). We use a Gaussian signal distribution plus the ARGUS background function [12] for the M_{bc} distribution. The signal shape parameters are determined from MC. The background parameters are obtained simultaneously in the fit to data. The ΔE distribution is modeled by a double Gaussian signal function plus a linear background function. We obtain shape parameters separately for candidates with and without $D^{*+} \rightarrow D^+\pi^0$ decays to account for small differences between the two cases.

The fit yields 130 ± 13 signal events, where 20% include $D^{*+} \rightarrow D^+\pi^0$ decays. To obtain the branching fraction $\mathcal{B}(B^0 \rightarrow D^{*+}D^{*-})$, we use the reconstruction efficiency and the known branching fraction for each subdecay mode. We obtain an effective efficiency of $[1.06 \pm 0.08] \times 10^{-3}$ from the sum of the products of MC reconstruction efficiencies and branching fractions for each of the subdecays. Small corrections are applied to the reconstruction efficiencies for charged tracks, neutral pions and K_S^0 mesons to account for differences between data and MC.

We obtain

$$\mathcal{B}(B^0 \rightarrow D^{*+}D^{*-}) = [0.81 \pm 0.08(\text{stat}) \pm 0.11(\text{syst})] \times 10^{-3}, \quad (2)$$

where the first error is statistical and the second is systematic. The result is consistent with the present world-average value [13].

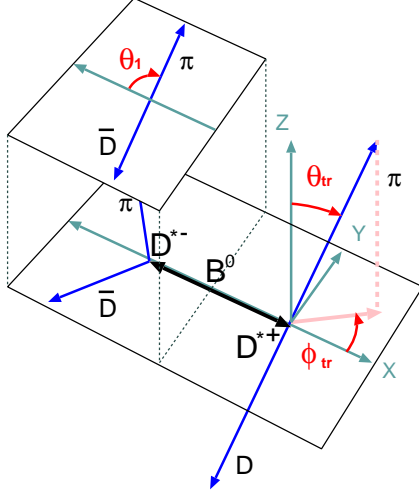


Fig. 2. Definition of the angles in the transversity basis. Angle θ_{tr} and ϕ_{tr} are defined in the D^{*+} rest frame (the lower plane), while θ_1 is defined in the D^{*-} rest frame (the upper plane).

The dominant sources of the systematic error are uncertainties in the tracking efficiency (11%) and in the subdecay branching fractions (7%). Other sources are uncertainties in the fit parameters and methods (1%), in the reconstruction efficiencies of π^0 (2%) and K_S^0 (1%), particle identification (1%), polarization parameters (2%), the number of B mesons (1%), and MC statistics (1%), where each value in parentheses is the total contribution.

4 Polarization

The time-dependent CP analysis requires knowledge of the CP -odd fraction. To obtain the CP -odd fraction without bias, we must take into account the efficiency difference between the two CP -even components. Therefore, we perform a time-integrated two-dimensional angular analysis to obtain the fraction of each polarization component. We use the transversity basis [14] where three angles θ_1 , θ_{tr} and ϕ_{tr} are defined in Fig. 2. The angle θ_1 is the angle between the momentum of the slow pion from the D^{*-} in the D^{*-} rest frame and the direction opposite to B momentum in the D^{*-} rest frame. The angle θ_{tr} is the polar angle between the normal to the D^{*-} decay plane and the direction of flight of the slow pion from the D^{*+} in the D^{*+} rest frame. The angle ϕ_{tr} is the corresponding azimuthal angle, where $\phi_{\text{tr}} = 0$ is the direction antiparallel to the D^{*-} flight direction. Integrating over time and the angle ϕ_{tr} , the two-dimensional differential decay rate is

$$\frac{1}{\Gamma} \frac{d^2\Gamma}{d \cos \theta_{\text{tr}} d \cos \theta_1} = \frac{9}{16} \sum_{i=0,||,\perp} R_i H_i(\cos \theta_{\text{tr}}, \cos \theta_1), \quad (3)$$

where $i = 0, \parallel$, or \perp denotes longitudinal, transverse parallel, or transverse perpendicular components, R_i is its fraction that satisfies

$$R_0 + R_{\parallel} + R_{\perp} = 1, \quad (4)$$

and H_i is its angular distribution defined as

$$\begin{aligned} H_0(\cos \theta_{\text{tr}}, \cos \theta_1) &= 2 \sin^2 \theta_{\text{tr}} \cos^2 \theta_1, \\ H_{\parallel}(\cos \theta_{\text{tr}}, \cos \theta_1) &= \sin^2 \theta_{\text{tr}} \sin^2 \theta_1, \\ H_{\perp}(\cos \theta_{\text{tr}}, \cos \theta_1) &= 2 \cos^2 \theta_{\text{tr}} \sin^2 \theta_1. \end{aligned} \quad (5)$$

The fraction R_{\perp} corresponds to the CP -odd fraction.

Eq. (3) is affected by the detector efficiency, in particular due to the correlations between transversity angles and slow pion detection efficiencies. To take these effects into account, we replace $H_i(\cos \theta_{\text{tr}}, \cos \theta_1)$ with distributions of reconstructed MC events $\mathcal{H}_i(\cos \theta_{\text{tr}}, \cos \theta_1)$, which are prepared separately for candidates with and without $D^{*+} \rightarrow D^+ \pi^0$ decays as is done in the branching fraction measurement. We also introduce effective polarization parameters $R'_i \equiv \epsilon_i R_i / (\epsilon_0 R_0 + \epsilon_{\parallel} R_{\parallel} + \epsilon_{\perp} R_{\perp})$, where ϵ_i is a total reconstruction efficiency for each transversity amplitude. As a result, the signal probability density function (PDF) for the fit is defined as

$$\mathcal{H}_{\text{sig}} = \sum_i R'_i \mathcal{H}_i(\cos \theta_{\text{tr}}, \cos \theta_1). \quad (6)$$

We determine the following likelihood value for each event:

$$\mathcal{L} = f_{\text{sig}} \mathcal{H}_{\text{sig}} + (1 - f_{\text{sig}}) \mathcal{H}_{\text{bg}}, \quad (7)$$

where f_{sig} is the signal probability calculated on an event-by-event basis as a function of ΔE and M_{bc} . The background PDF \mathcal{H}_{bg} is determined from the sideband region ($5.20 \text{ GeV}/c^2 < M_{\text{bc}} < 5.26 \text{ GeV}/c^2$, $|\Delta E| < 0.2 \text{ GeV}$). A fit that maximizes the product of the likelihood values over all events yields

$$\begin{aligned} R_{\perp} &= 0.19 \pm 0.08(\text{stat}) \pm 0.01(\text{syst}), \\ R_0 &= 0.57 \pm 0.08(\text{stat}) \pm 0.02(\text{syst}). \end{aligned} \quad (8)$$

Figure 3 shows the angular distributions with the results of the fit.

We study the uncertainties of the following items to determine the systematic errors: background shape parameters, angular resolutions, and slow pion detection efficiencies. Also included are a possible fit bias, MC histogram bin size

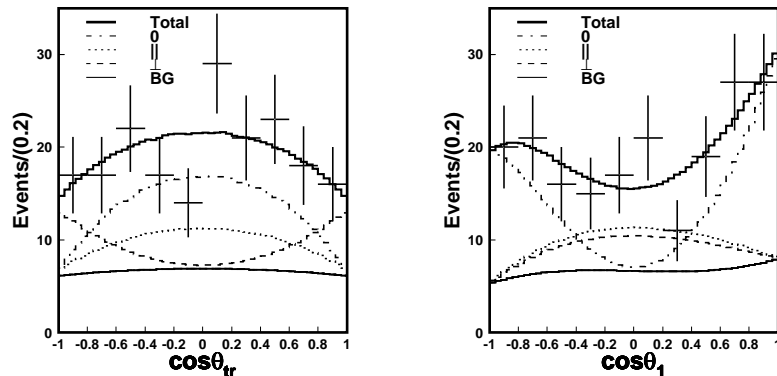


Fig. 3. Angular distributions of the $B^0 \rightarrow D^{*+}D^{*-}$ candidates in (left) $\cos \theta_{\text{tr}}$ and (right) $\cos \theta_1$ projections. In each figure, the dot-dashed, dotted and dashed lines correspond to longitudinal, transverse parallel and transverse perpendicular polarization components, respectively. The thin solid line is the background, and the thick solid line shows the sum of all contributions. The asymmetry in the $\cos \theta_1$ distribution is due to the inefficiency for low momentum track reconstruction.

dependence and misreconstruction effects. These systematic errors are much smaller than the statistical errors.

5 CP Asymmetries

We perform an unbinned maximum likelihood fit to the three dimensional Δt , $\cos \theta_{\text{tr}}$ and $\cos \theta_1$ distributions for $B^0 \rightarrow D^{*+}D^{*-}$ candidates to measure the CP -violation parameters.

The B^0 meson decay vertices are reconstructed using the D meson trajectory and an IP constraint. We do not use slow pions from D^{*+} decays. We require that at least one D meson has two or more daughter tracks with a sufficient number of the SVD hits to precisely measure the D meson trajectory. The f_{tag} vertex determination is the same as for other CP -violation measurements [4].

The b -flavor of the accompanying B meson is identified from inclusive properties of particles that are not associated with the reconstructed $B^0 \rightarrow f_{CP}$ decay [3]. We use two parameters, q and r , to represent the flavor tagging information. The first, q , is already defined in Eq. (1). The parameter r is an event-by-event, MC-determined flavor-tagging dilution factor that ranges from $r = 0$ for no flavor discrimination to $r = 1$ for unambiguous flavor assignment. This assignment is used only to sort data into six r intervals. The wrong tag fractions for the six r intervals, w_l ($l = 1, 6$), and differences between B^0 and \bar{B}^0 decays, Δw_l , are determined from the data; we use the same values that were used for the $\sin 2\phi_1$ measurement [4].

The signal PDF is given by

$$\mathcal{P}_{\text{sig}} = \frac{e^{-|\Delta t|/\tau_{B^0}}}{4\tau_{B^0}} \sum_{i=0,\parallel,\perp} R'_i \mathcal{H}_i(\cos \theta_{\text{tr}}, \cos \theta_1) \times \left[1 - q\Delta w + q(1 - 2w)(\mathcal{A} \cos \Delta m \Delta t + \xi_i \mathcal{S} \sin \Delta m \Delta t) \right], \quad (9)$$

where CP parity ξ_i is $+1$ for $i = 0$ and \parallel , and -1 for $i = \perp$. We assume universal CP -violation parameters in Eq. (9), i.e. $\mathcal{S}_0 = \mathcal{S}_{\parallel} = \mathcal{S}_{\perp}$ and $\mathcal{A}_0 = \mathcal{A}_{\parallel} = \mathcal{A}_{\perp}$. The distribution is convolved with the proper-time interval resolution function $R_{\text{sig}}(\Delta t)$ [4], which takes into account the finite vertex resolution.

We determine the following likelihood value for the j -th event:

$$P_j = (1 - f_{\text{ol}}) \int \left[f_{\text{sig}} \mathcal{P}_{\text{sig}}(\Delta t') R_{\text{sig}}(\Delta t_i - \Delta t') + (1 - f_{\text{sig}}) \mathcal{P}_{\text{bkg}}(\Delta t') R_{\text{bkg}}(\Delta t_i - \Delta t') \right] d(\Delta t') + f_{\text{ol}} P_{\text{ol}}(\Delta t_i), \quad (10)$$

where $P_{\text{ol}}(\Delta t)$ is a broad Gaussian function that represents an outlier component [3] with a small fraction f_{ol} . The f_{sig} calculation is explained in the previous section. The PDF for background events, $\mathcal{P}_{\text{bkg}}(\Delta t)$, is expressed as a sum of exponential and prompt components, and is convolved with R_{bkg} that is a sum of two Gaussians. All parameters in $\mathcal{P}_{\text{bkg}}(\Delta t)$ and R_{bkg} are determined by a fit to the Δt distribution of a background-enhanced control sample; i.e. events outside of the $\Delta E - M_{\text{bc}}$ signal region. We fix τ_{B^0} and Δm_d to their world-average values [13]. The only free parameters in the final fit are \mathcal{S} and \mathcal{A} , which are determined by maximizing the likelihood function $L = \prod_j P_j(\Delta t_j, \cos \theta_{\text{tr}j}, \cos \theta_{1j}; \mathcal{S}, \mathcal{A})$, where the product is over all events. The fit yields

$$\begin{aligned} \mathcal{S} &= -0.75 \pm 0.56(\text{stat}) \pm 0.12(\text{syst}), \\ \mathcal{A} &= -0.26 \pm 0.26(\text{stat}) \pm 0.06(\text{syst}), \end{aligned} \quad (11)$$

where the first errors are statistical and the second errors are systematic. These results are consistent with the SM expectations for small penguin contributions.

We define the raw asymmetry in each Δt bin by $(N_{q=+1} - N_{q=-1}) / (N_{q=+1} + N_{q=-1})$, where $N_{q=+1(-1)}$ is the number of observed candidates with $q = +1(-1)$. Figure 4 shows the raw asymmetries in two regions of the flavor-tagging parameter r . While the numbers of events in the two regions are similar, the effective tagging efficiency is much larger and the background dilution is smaller in the region $0.5 < r \leq 1.0$. Note that these projections onto

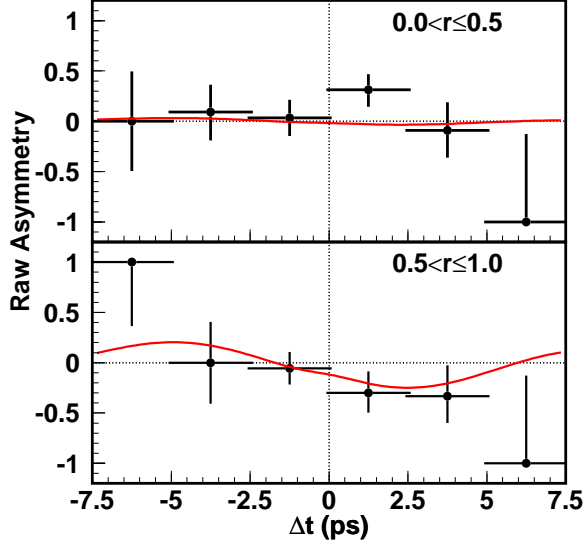


Fig. 4. Raw $B^0 \rightarrow D^{*+}D^{*-}$ asymmetry in bins of Δt for (top) $0 < r \leq 0.5$ and $0.5 < r \leq 1.0$ (bottom). The solid curves show the result of the unbinned maximum-likelihood fit.

the Δt axis do not take into account event-by-event information (such as the signal fraction, the wrong tag fraction and the vertex resolution), which are used in the unbinned maximum-likelihood fit.

The sources of the systematic errors include uncertainties in the vertex reconstruction (0.05 for \mathcal{S} and 0.03 for \mathcal{A}), in the flavor tagging (0.04 for \mathcal{S} and 0.02 for \mathcal{A}), in the resolution function (0.05 for \mathcal{S} and 0.01 for \mathcal{A}), in the background fractions (0.04 for \mathcal{S} and 0.02 for \mathcal{A}), in the tag-side interference [4] (0.01 for \mathcal{S} and 0.03 for \mathcal{A}), and in the polarization parameters (0.06 for \mathcal{S} and 0.01 for \mathcal{A}). Other contributions for \mathcal{S} come from a possible fit bias (0.04) and from uncertainties in τ_{B^0} and Δm_d (0.02). We add each contribution in quadrature to obtain the total systematic uncertainty.

We perform various cross checks. A fit to the same sample with \mathcal{A} fixed at zero yields $\mathcal{S} = -0.69 \pm 0.56(\text{stat})$. We check with an ensemble of MC pseudo-experiments that the fit has no sizable bias and the expected statistical errors are consistent with the measurement. We also select the following decay modes that have similar properties to the $B^0 \rightarrow D^{*+}D^{*-}$ decay: $B^0 \rightarrow D^{*-}D_s^{*+}$, $D^-D_s^{*+}$, $D^{*-}D_s^+$, $D^-D_s^+$, and $B^+ \rightarrow \bar{D}^{*0}D_s^{*+}$, $\bar{D}^0D_s^{*+}$, $\bar{D}^{*0}D_s^+$ and $\bar{D}^0D_s^+$. Fits to the control samples yield $\mathcal{S}[B^0 \rightarrow D^{(*)}D_s^{(*)}] = -0.12 \pm 0.08$, $\mathcal{A}[B^0 \rightarrow D^{(*)}D_s^{(*)}] = +0.02 \pm 0.05$, $\mathcal{S}[B^+ \rightarrow D^{(*)}D_s^{(*)}] = -0.10 \pm 0.07$, and $\mathcal{A}[B^+ \rightarrow D^{(*)}D_s^{(*)}] = -0.001 \pm 0.050$, where errors are statistical only. All results are consistent with zero. We also measure the B meson lifetime using $B^0 \rightarrow D^{*+}D^{*-}$ candidates as well as the control samples. All results are consistent with the present world-average values. A fit to the Δt distribution of the $B^0 \rightarrow$

$D^{*+}D^{*-}$ without using polarization angle information yields $\mathcal{S} = -0.57 \pm 0.45$, $\mathcal{A} = -0.29 \pm 0.26$; this result suggests that the CP -odd component is small, supporting our polarization measurement.

Although the statistics are not sufficient to provide tight constraints, we also consider polarization-dependent values for \mathcal{S} and \mathcal{A} , which may arise from possible differences in the contributions of the penguin diagrams. We assume that the CP asymmetries for the CP -odd component are consistent with the SM expectations, and fix \mathcal{S}_\perp at the world-average value of $\sin 2\phi_1$ [13] and \mathcal{A}_\perp at zero. A fit with this assumption yields $\mathcal{S} = -0.72 \pm 0.50$ and $\mathcal{A} = -0.42 \pm 0.30$ for the CP -even component, also consistent with the SM expectations.

6 Conclusion

In summary, we have performed measurements of the branching fraction, the polarization parameters and the CP -violation parameters for $B^0 \rightarrow D^{*+}D^{*-}$ decays. The results are

$$\begin{aligned}
 \mathcal{B}(B^0 \rightarrow D^{*+}D^{*-}) &= [0.81 \pm 0.08(\text{stat}) \pm 0.11(\text{syst})] \times 10^{-3}, \\
 R_\perp &= 0.19 \pm 0.08(\text{stat}) \pm 0.01(\text{syst}), \\
 R_0 &= 0.57 \pm 0.08(\text{stat}) \pm 0.02(\text{syst}), \\
 \mathcal{S} &= -0.75 \pm 0.56(\text{stat}) \pm 0.12(\text{syst}), \\
 \mathcal{A} &= -0.26 \pm 0.26(\text{stat}) \pm 0.06(\text{syst}).
 \end{aligned} \tag{12}$$

The polarization parameters and CP -violation parameters are consistent with the SM expectations and theoretical predictions for small penguin contributions [15].

Acknowledgments

We thank the KEKB group for the excellent operation of the accelerator, the KEK Cryogenics group for the efficient operation of the solenoid, and the KEK computer group and the NII for valuable computing and Super-SINET network support. We acknowledge support from MEXT and JSPS (Japan); ARC and DEST (Australia); NSFC (contract No. 10175071, China); DST (India); the BK21 program of MOEHRD and the CHEP SRC program of KOSEF (Korea); KBN (contract No. 2P03B 01324, Poland); MIST (Russia); MESS (Slovenia); NSC and MOE (Taiwan); and DOE (USA).

References

- [1] M. Kobayashi and T. Maskawa, *Prog. Theor. Phys.* **49**, 652 (1973).
- [2] A. B. Carter and A. I. Sanda, *Phys. Rev. D* **23**, 1567 (1981); I. I. Bigi and A. I. Sanda, *Nucl. Phys.* **B193**, 85 (1981).
- [3] Belle Collaboration, K. Abe *et al.*, *Phys. Rev. Lett.* **87**, 091802 (2001); *Phys. Rev. D* **66**, 032007 (2002); *Phys. Rev. D* **66**, 071102 (2002).
- [4] Belle Collaboration, K. Abe *et al.*, hep-ex/0408111.
- [5] BaBar Collaboration, B. Aubert *et al.*, *Phys. Rev. Lett.* **87**, 091801 (2001); *Phys. Rev. D* **66**, 032003 (2002); *Phys. Rev. Lett.* **89**, 201802 (2002).
- [6] Throughout this paper, the inclusion of the charge conjugate decay mode is implied unless otherwise stated.
- [7] X. Y. Pham and Z. Z. Xing, *Phys. Lett. B* **458**, 375 (1999).
- [8] BaBar Collaboration, B. Aubert *et al.*, *Phys. Rev. Lett.* **91**, 131801 (2003).
- [9] S. Kurokawa and E. Kikutani, *Nucl. Instrum. Methods A* **499**, 1 (2003).
- [10] Belle Collaboration, A. Abashian *et al.*, *Nucl. Instrum. Methods A* **479**, 117 (2002).
- [11] G. C. Fox and S. Wolfram, *Phys. Rev. Lett.* **41**, 1581 (1978).
- [12] ARGUS Collaboration, H. Albrecht *et al.*, *Phys. Lett. B* **241**, 278 (1990).
- [13] Particle Data Group, K. Hagiwara *et al.*, Particle Listings in the 2003 Review of Particle Physics, http://www-pdg.lbl.gov/2003/contents_listings.html.
- [14] I. Dunietz, H. R. Quinn, A. Snyder, W. Toki and H. J. Lipkin, *Phys. Rev. D* **43**, 2193 (1991).
- [15] If penguin contributions are small, the theoretical predictions within the SM are $\mathcal{A} \simeq 0$ and $\mathcal{S} \simeq -\sin 2\phi_1$, where $\sin 2\phi_1$ is measured in $b \rightarrow c\bar{c}s$ transitions to be 0.731 ± 0.056 [13].